Wind driven currents in the Channel of São Sebastião: winter, 1979

Belmiro Mendes de CASTRO Fo.

Instituto Oceanográfico da Universidade de São Paulo
(Caixa Postal 9075, 01051 São Paulo, SP)

● *Abstract:* Simultaneous 40 h low-passed wind, current and sea level data in the Channel of São Sebastião (CSS) and atmospheric pressure and sea level data in the South Brazil Bight (SBB) during winter of 1979 were analysed and compared. Currents in the CSS were predominantly northeastward, associated with frontal southerly winds. Current reversals occurred between meteorological disturbance passages. There were significant correlation between alongchannel components of wind and current, with a time lag of 12-18 h, wind leading; and between alongchannel component of current and sea level, with a time lag of 6-12 h, current leading. Most of the variance in the CSS series is concentrated in two frequency bands: 11-16 d and 3 d. SBB series also show high variance in those two bands. Coherences in those two bands show significant values when calculated between alongchannel components of wind and current, and sea level, in the CSS. Those three last signals were almost in phase in the 11-16 d band; and there was a lead of 16 h (25 h) by wind over current (sea level) in the 3 d band. There are several indications that in the subtidal band currents in the CSS are not totally locally forced.

● *Descriptors:* Wind-driven currents, Sea level, Canal de São Sebastião, Continental shelves, Brazil.

● *Descritores:* Correntes induzidas pelo vento, Nível do mar, Canal de São Sebastião: SP, Plataforma continental, Brasil.

Introduction

The Channel of São Sebastião (CSS) is located along the southeast coast of Brazil, at 23° S, between the continent and the Island of São Sebastião (Fig. 1). The southern and northern entrances to the channel are 7.2 km and 5.6 km wide, respectively, while the center of the channel is about 1.9 km wide. Although the southern and northern entrances have similar width, there is a large shallow region, about 3.7 km wide, in the eastern part of the latter. The main channel characterized by abrupt bottom slopes at the margins, and depths greater than 20 m along its longitudinal axis, is about 22 km long and has a crescent moon shape. The maximum depth, located in the middle of the channel, is 50 m.

The CSS is part of the South Brazil Bight (SBB), which itself is the part of the Brazilian continental shelf delimited by Cabo Frio (23° S) and Cabo de Santa Marta (28° 40' S) on the coast (Fig. 2).

There are few works about currents in the CSS. Emilsson (1962) analysed preliminarly 13 days of current data from a mooring deployed near the center of the channel. He found no correlation between currents and tides, and speculated that the low amplitude of tidal current is due to the fact that the semi-diurnal tidal wave, coming from E-SE, reaches both extremities of the channel at the same time, the result being a negligible tidal transport. Currents were, on the other hand, highly influenced by the wind: winds from the south forced northeastward currents, while winds from the north forced southwestward currents.

Kvinge (1967) analysed more carefully the same data set collected by Emilsson (1962), and reached similar conclusions. Kvinge (*op. cit.*) compared tidal currents to wind driven currents and found maximum speeds of 0.08 m/s for the semi-diurnal component, and of 0.60 m/s for the wind driven component. Periods of 4 days for current, and of 4-5 days for atmospheric pressure and sea level were found. Kvinge (1967) then inferred that current oscillations should be associated to wind oscillations due to meteorological frontal systems.
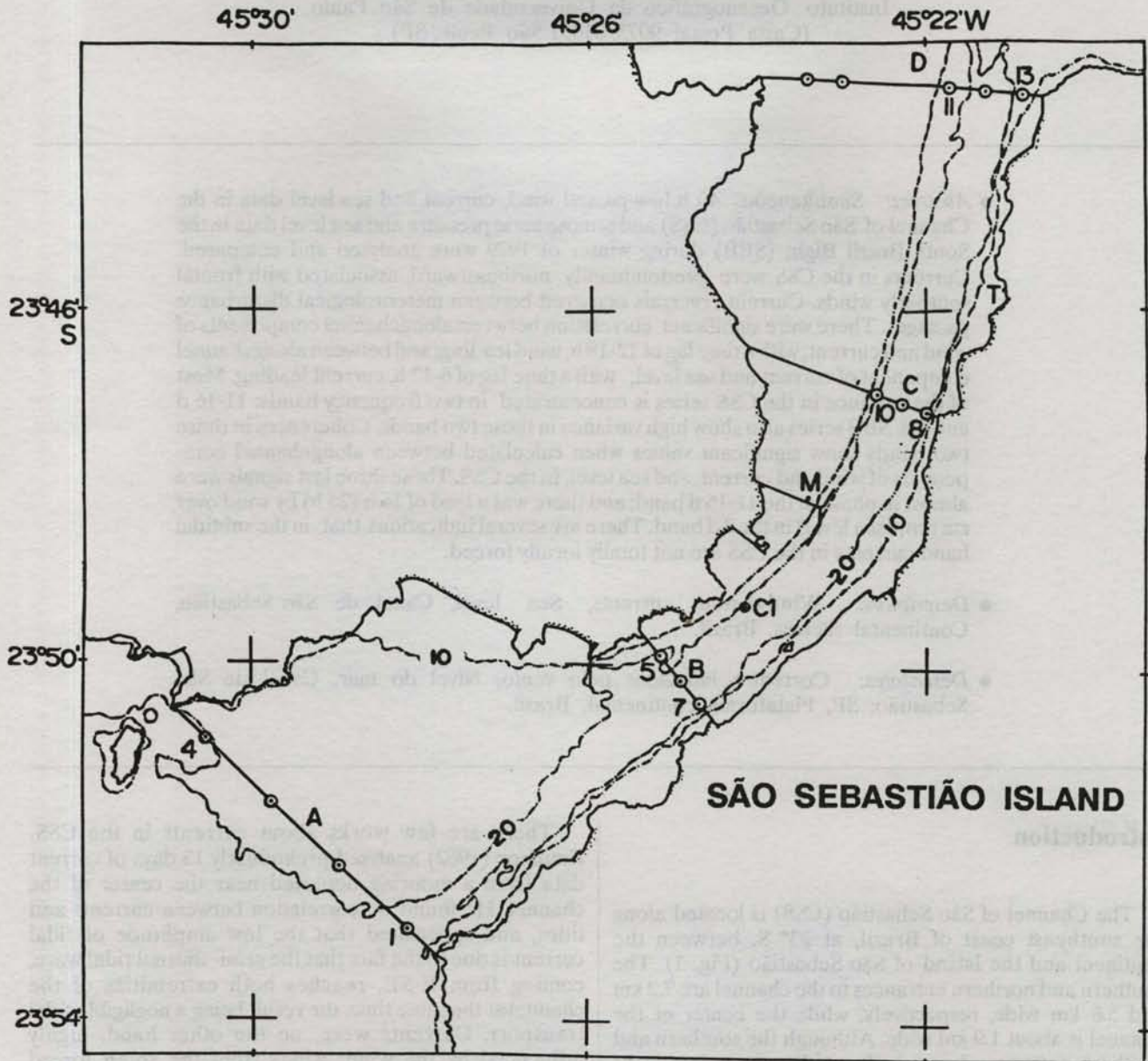
Fig. 1. Channel of São Sebastião showing hydrographic stations (1 to 13), current stations (C1 and 8), meteorological station (M) and tidal station (T). Depths are in meters.
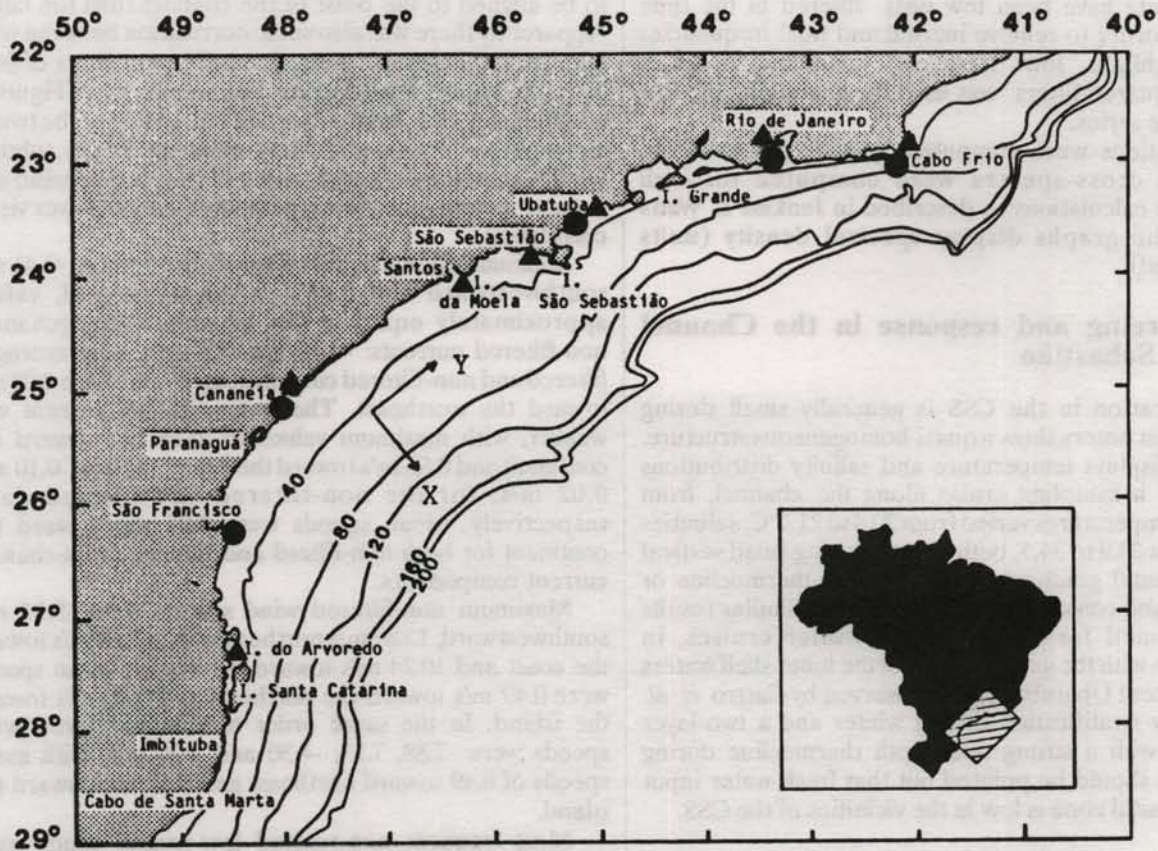
Fig. 2. South Brazil Bight showing depths in meters, tidal stations (circles) and meteorological stations (triangles). X and Y axis show the orientation used for decomposing vectors.

Castro (1985) applied a barotropic nested numerical model to study wind driven circulation in the SBB. A hierarchy of three grids was used, the higher resolution grid covering the CSS. An experiment that used a 10 day wind data set from the National Meteorological Center (U.S.A.) suggested that currents in the CSS are not, in general, forced locally.

The objective of this work is to analyse the winter wind forcing and subtidal response of the CSS waters based upon a more comprehensive data set. First, the data set and the methods used are presented. In sequence, subtidal variability in the CSS is described, and then the large scale subtidal variability in the SBB is introduced.

Data set and methods

A time series of current from point C1 in the CSS (Fig. 1) was analysed. A single one current meter mooring was deployed for a period of 47 days, from 8/20/79, 0 h to 10/5/79, 23 h (these and all subsequent time references are in GMT; Local Time = GMT - 3 h). Local depth at point

C1 is 25 m, and the current meter was located 5 m below the surface (wave activity at point C1 is restricted by the shape of the channel). Shorter time series of currents at point 8 (Fig. 1) were also analysed.

Data were available also for the variables coastal sea level and atmospheric pressure, for stations located in Cabo Frio (CF), Rio de Janeiro (RJ), Ubatuba (UB), São Sebastião (SS), Moela (MO), Cananéia (CA), São Francisco (SF) and Arvoredo (AR). Not all the stations have both meteorological and tidal observations. The positions and types of stations are shown in Figure 2. A 95 day subset was chosen to be used in the analysis: from 7/15/79, 0 h, to 10/17/79, 23 h.

One gap, length of 9 days, in the sea level data for UB, was filled by values calculated from frequency band linear regressions of sea level data between RJ and UB. The same method was used to fill two other gaps:

a) one gap, length of 2 days, in the sea level data for UB. Base station used: RJ;

b) one gap, length of 9 days, in the air pressure data for UB. Base station used: SS.

Observations of meteorological data for CF are not evenly spaced in time: there are three observations per day, at 0 h, 12 h and 18 h. A four point Lagrangean interpolation was used to fill in the missing observations.

All data have been low pass filtered in the time domain in order to remove inertial and tidal frequencies and to highlight low frequency variations. A set of Lanczos squared filters was used for generating the low passed time series.

Correlations were computed by standard methods. Auto and cross-spectra were computed through correlation calculations as described in Jenkins & Watts (1968). The graphs display spectral density (units squared/cpd).

Local forcing and response in the Channel of São Sebastião

Stratification in the CSS is generally small during winter, when waters show a quasi-homogeneous structure. Figure 3 displays temperature and salinity distributions from an 8 h sampling cruise along the channel, from 8/21/79. Temperatures varied from 20.4 to 21.2°C; salinities varied from 33.9 to 34.5, both fields showing small vertical and horizontal gradients. There is no thermocline or halocline, and consequently no picnocline. Similar results were attained for several other winter cruises, in accordance with the general trend of the inner shelf waters in the adjacent Ubatuba region, observed by Castro *et al.* (1987): low stratification during winter and a two-layer character, with a strong mid-depth thermocline during summer. It should be pointed out that fresh water input into the coastal zone is low in the vicinities of the CSS.

The quasi-homogeneity during winter confers a dominant barotropic mode type of response to the CSS waters. Figure 4 shows progressive vector diagrams from 13 h of hourly current data collected at station 8 (Fig. 1), at three depths. As it can be observed, the vertical shear of currents was small, reflecting the quasi-barotropic nature of the CSS waters for this time of the year.

Some statistical parameters for sea level oscillations and for rotated alongchannel and crosschannel components of wind at SS and of current at point C1 are shown in Table 1. Angle of rotation is 51.5°, clockwise, so vector components are either parallel or normal to the main axis of the channel. Variance reduction due to the 40 h low pass filtering was small (about 12 %) for the alongchannel current component, confirming the small amplitude of tidal current. The variance of the low-passed crosschannel current is about 1 % of the variance of the low-passed alongchannel current, reflecting the almost rectilinear current variability at the point of observation. Events with periods greater than 40 h accounted for 58 % of the alongchannel and for 44 % of the crosschannel wind variance. The reductions of about half in the variance for the wind components reflect the importance of the sea-breeze in the wind signal. For sea level, on the other hand, variance reduction was about 81 %, showing that sea level oscillations are dominated by tidal oscillations.

Time distributions of 40 h low-passed sea level and non-rotated current and wind vectors are shown in Figure

5. The high correlation between wind and current can be observed: wind events were followed, some time latter, by current events. Current vectors are not parallel to wind vectors, since the former vectors have a higher tendency to be aligned to the coast of the channel than the latter. Apparently there was also some correlation between wind and sea level signals. Alongchannel components of both 40 h low-passed wind and current are shown in Figure 6, confirming the high correlation existent between atmospheric forcing and water response in the subtidal band. Crosschannel components of low-passed wind and current vectors (not shown) presented a much lower visual correlation.

Maximum alongchannel filtered current was -0.41 m/s southwestward and 0.46 m/s northeastward, values approximately equal to the maximum alongchannel non-filtered currents: -0.45 and 0.54 m/s. The averaged filtered and non-filtered current speeds were both 0.08 m/s toward the northeast. The cross-channel current was weaker, with maximum values of -0.18 m/s toward the continent and 0.08 m/s toward the island, and of -0.10 and 0.02 m/s, for the non-filtered and filtered data, respectively. Mean speeds were 0.02 m/s toward the continent for both non-filterd and filtered cross-channel current components.

Maximum non-filtered wind speeds were -9.25 m/s southwestward, 13.87 m/s northeastward, -7.64 m/s toward the coast and 10.24 m/s toward the island. Mean speeds were 0.49 m/s toward the northeast and 0.76 m/s toward the island. In the same order maximum filtered wind speeds were -7.88, 7.35, -4.30 and 5.26 m/s, with mean speeds of 0.49 toward northeast and 0.65 m/s toward the island.

Most frequent non-rotated low-passed winds were blowing toward 140-180°, representing 39 % of the observations; and toward 0-40°, representing 37 % of the observations (Fig. 7b). Mean speeds were slightly lower (3.2 m/s) for the 140-180° wind than for the 0-40° wind (4.2 m/s) (Fig. 7a), implying in a total displacement of 4434 km for the first block and of 4664 km for the second block. Thus, although less frequent, the 0-40° wind imparted slightly more kinetic energy to the sea waters than the 140-180° wind. Most frequent non-rotated low-passed currents (Fig. 7d) were toward 30-60°, representing 59 % of the observations, with the absolute maximum toward 50° comprising 38 % of the observed values; and toward 240-250°, representing 38 % of the observations. Mean speeds (Fig. 7c) were higher for the 30-60° (0.27 m/s for 50°) than for the 240-250° current (0.15 m/s), showing that northeastward mass transport at station C1 was approximatelly 2.5 times higher than the southwestward mass transport.

The almost equal frequency of southeastward and northeastward winds, and the predominance of northeastward currents are shown again in Figure 8. Although non-rotated current vectors were mainly to the northeast, nine episodes of southwestward water motion occurred, which were present also in the wind signal. Northeastward winds and currents may be associated with the passage of meteorological synoptic systems, which are frequent and intense in the region during winter and spring. Current reversals should be associated with wind reversals, which blows toward southeast during normal non frontal situations.
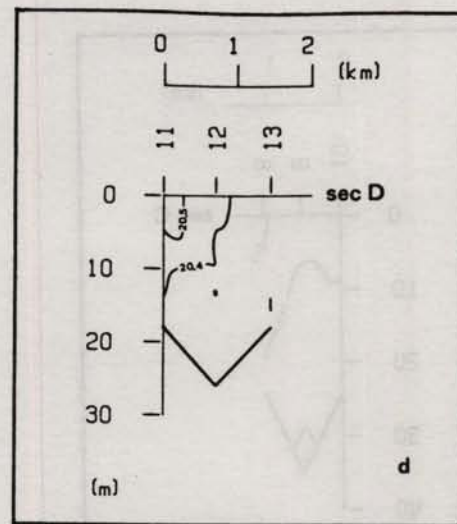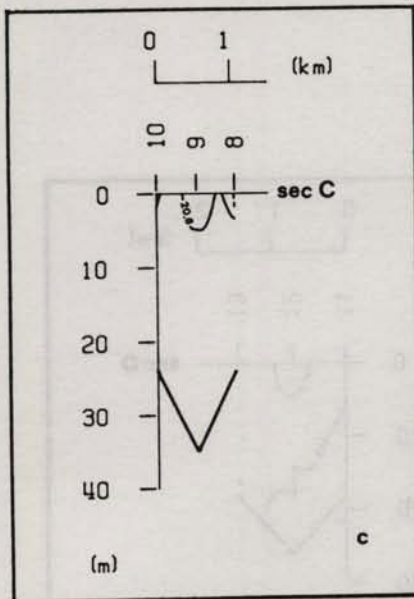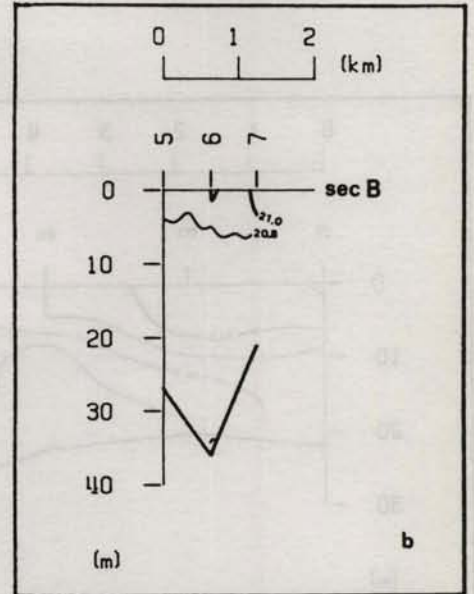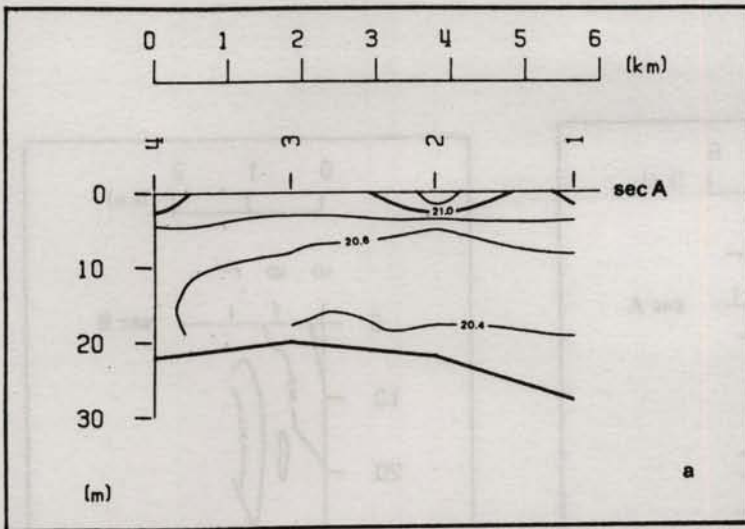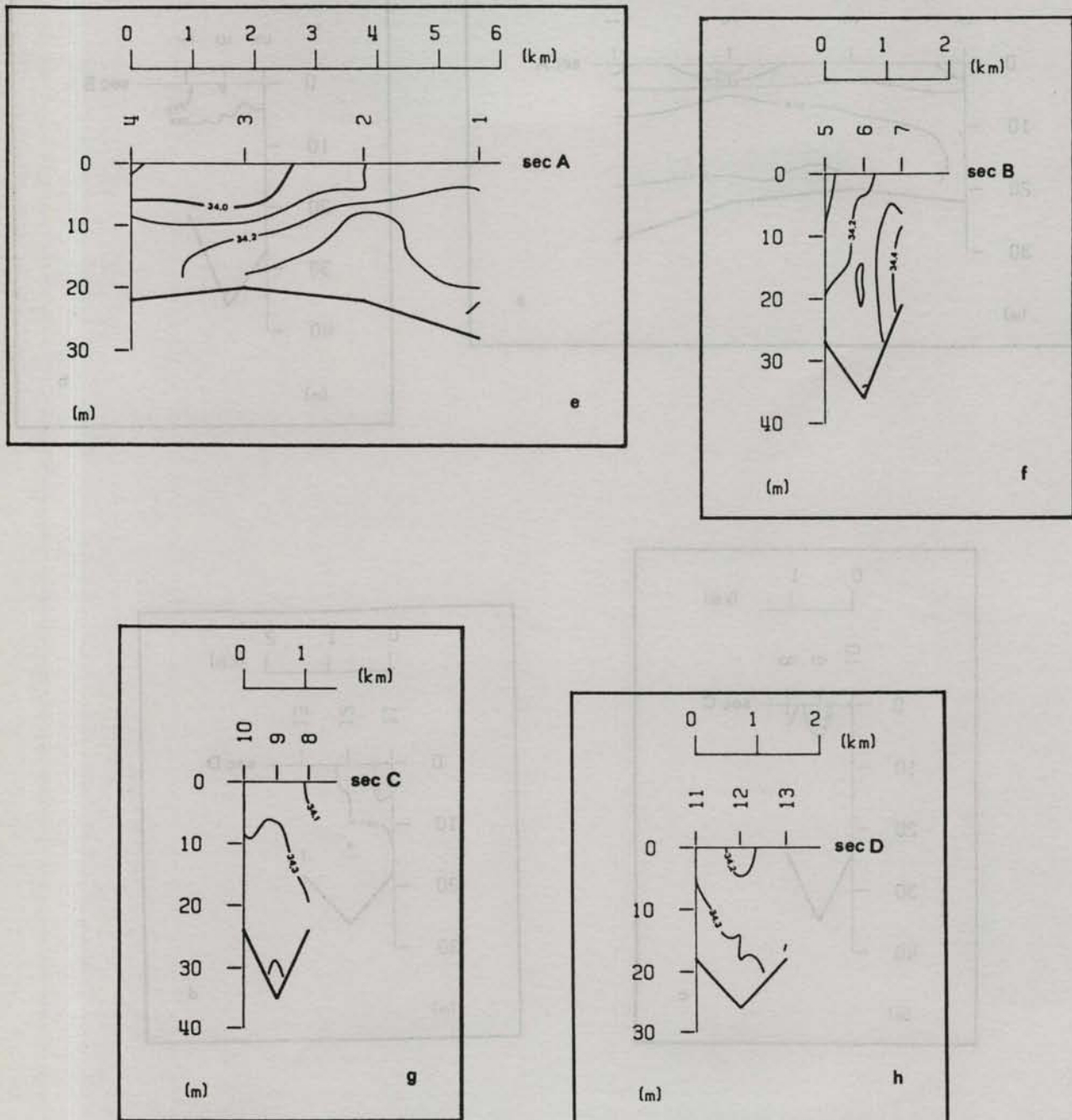
(Cont.)

Fig. 3. Vertical distribution of temperature (a, b, c and d) and salinity (e, f, g and h) in sections A, B, C and D, respectively (see Figure 1 for section location).
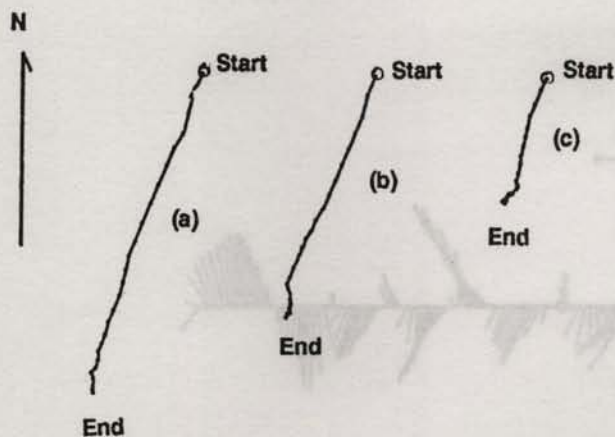
Fig. 4. Progressive vector diagrams of current at point 8 (see Fig. 1): (a) 2 m; (b) 12 m; and (c) 27 m depth. Start: 10/23/78, 17 h; end: 10/24/78, 18 h.

Correlation calculations between the filtered alongchannel components of the vector time series, wind and current, show a time lag of 12-18 h, wind leading current (Fig. 9a). Correlations higher than 0.35 are significant at a 95 % level of confidence. Correlations between filtered alongchannel component of wind and sea level oscillations show a time lag of 24-30 h, wind leading (Fig. 9b); the 95 % level of confidence points to values near 0.37, so the signals were only marginally correlated. Time lag for maximum correlation between filtered alongchannel current component and sea level was between 6 and 12 h, current leading (Fig. 9c); correlations higher than 0.40 are significant at a 95 % level of confidence. The cross-channel component of the wind vector seemed to be also influencing the alongchannel current, with a time lag of 12-18 h, wind leading again (Fig. 9d); correlations higher than 0.34 are significant.

Results of spectral analysis for the low-pass filtered sea level and alongchannel components of wind and current are shown in Figure 10. The number of degrees of freedom in the spectral calculations is 7. The three autospectra show relative maxima of energy for frequencies between 0.09 and 0.06 cpd (11-16 d band), and 0.34 and 0.31 cpd (3 d band) (Figs 10a-10c), although the 3 d band relative maximum for sea level is only suggested. Coherences show significant values in the two period bands where the auto-spectra "peak": 11-16 d and 3 d (Figs 10d-10f). Phase calculations (Figs. 10g-10i) show that sea level and alongchannel wind and current were almost in phase at the 11-16 d band. In the 3 d band alongchannel wind leaded alongchannel current and sea level by about 16 h and 25 h, respectively; consequently current leaded sea level by about 10 h.

Large scale forcing and response in the South Brazil Bight

With the objective of inserting the CSS current data into a more general perspective, a statistical analysis of meteorological and sea level data in the SBB, for the winter of 1979, was conducted.

Synoptic scale meteorological disturbances, through air-sea interaction mechanisms, are an important source of energy for motions in the coastal ocean on the time scale of days to weeks. Those disturbances can be considered as perturbations in the mean meteorological conditions.

In the South Atlantic the main large scale atmospheric feature in the troposphere is the South Atlantic Anticyclone. Persistent during the whole year it strengthens during winter (July), and weakens during summer (January). The annual cycle of surface

Table 1. Time series statistics for data collected from 8/20/79 to 10/5/79. Values shown between brackets are percentages referred to the original data

Parameter	Mean	Min; Max	Variance Original	Low-passed
Sea level (m)	2.19	1.40; 2.92	0.1043	0.0198 (19)
Alongchannel wind (m/s)	0.49	-9.25; 13.87	11.5576	6.7237 (58)
Crosschannel wind (m/s)	0.76	-7.64; 10.24	12.1590	5.3002 (44)
Alongchannel current (m/s)	0.08	-0.45; 0.54	0.0465	0.0411 (88)
Crosschannel current (m/s)	-0.02	-0.18; 0.08	0.0011	0.0005 (45)

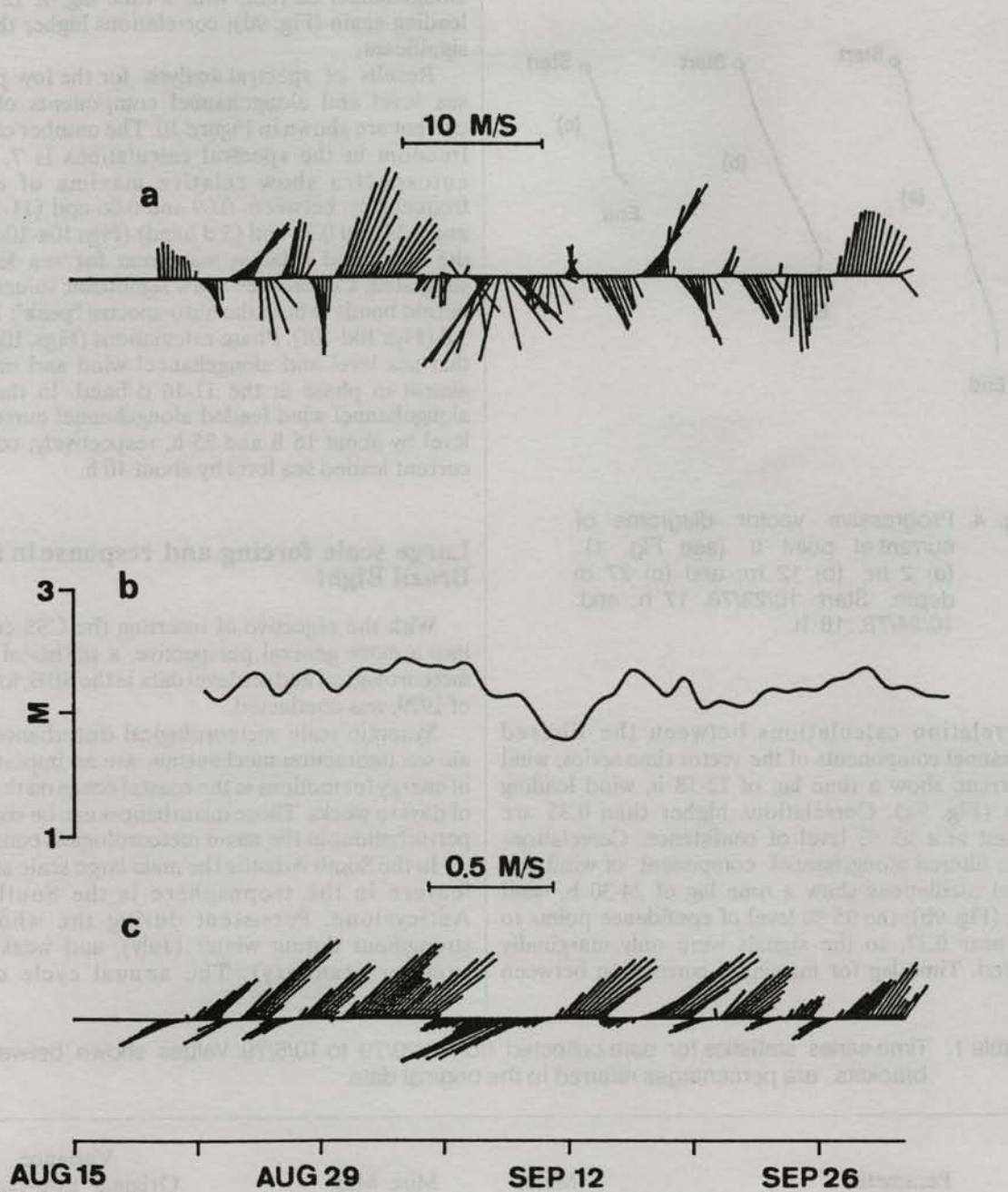## Large scale forcing and response in the South Brazil Bight

Fig. 5. Time distribution of 40 h low passed; (a) wind at point M; (b) sea level at point T; (c) current at point C1 (see Figure 1 for point location).
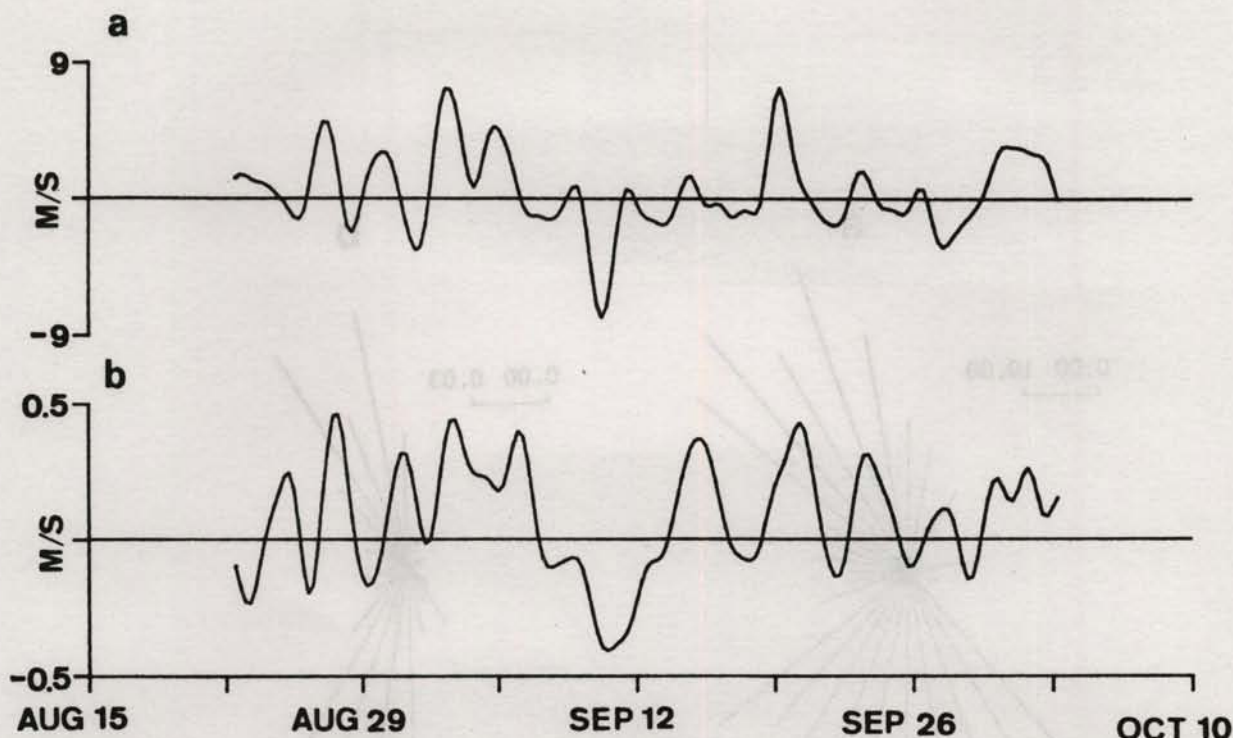
Fig. 6. Alongchannel components of 40 h low-passed; (a) wind at point M; (b) current at point C1 (see Figure 1 for point location).

atmospheric pressure is shown for two stations (Fig. 11): CA, covering 20 years of data (1956-76), and UB, covering 15 years of data (1961-75). A well defined annual wave shows higher values during winter and lower values during summer, following the advance of the South Atlantic Anticyclone over the continent during winter and its recession over the ocean during summer. The surface air temperature for those two stations also show a well defined annual wave (Fig. 11). The lower temperatures during winter reflect the penetration of polar air. The cold air is associated with migrating polar disturbances that originate in higher latitudes and move northeastward following the cold fronts.

An analysis of data published by Silva (1984) for the most frequent monthly winds at CA for the years 1956-75, reveals that during summer and during winter winds from E-SE and W-SW are the most frequent, respectively. The influence of the South Atlantic Anticyclone contributes to the predominance of easterlies during summer. Winds from the third quadrant, observed during winter, are generally associated with migrating polar disturbances.

The region is under the influence of the South Atlantic Anticyclone throughout the year, and immediately before the passage of the polar disturbance there is, in general, a low pressure trough associated with a cold front. Depending on the position of the migrating disturbance in relation to the coast at each moment, winds from different directions can affect the SBB. Typically a station in the region would experience a decline in surface pressure and winds from W-NW before the frontal passage, with an increase in surface pressure and winds rotating anticlockwise to southwest when the disturbance center approaches the station, followed by a decrease in surface pressure and northeasterly winds after the disturbance center passes.

In general, results from subtidal meteorological and coastal sea level data analysis for the SBB are similar to the results for the winter of 1978 (Castro, 1985). Surface atmospheric pressure fields may be used as tracers of meteorological disturbance passages. The 40 h low passed atmospheric pressure fields seem to be well correlated along the SBB coast (Fig. 12). Coherences between all stations and MO (Fig. 13a) are significant for a broad band between 3 and 16 d. Disturbances propagate northeastward along the coast from CA, with speeds of about 11 m/s and 20 m/s, for the 11-16 d and 3 d bands, respectively (Fig. 13b).

Low passed sea level data from several stations located along the SBB coast are shown in Figure 14. The signals present correlations higher than 0.6 at zero time lag. Disturbances propagate equatorward from SF, with mean phase speed of 18 m/s (Fig. 15). Coherency spectra between all the stations and a base station, UB, for example, show higher energies at 11-16 d, 8 d and 3 d periods (Fig. 16). Those disturbances propagate from CA to CF with mean speeds of 12 m/s, 22 m/s and 10 m/s, respectively (Fig. 16b).
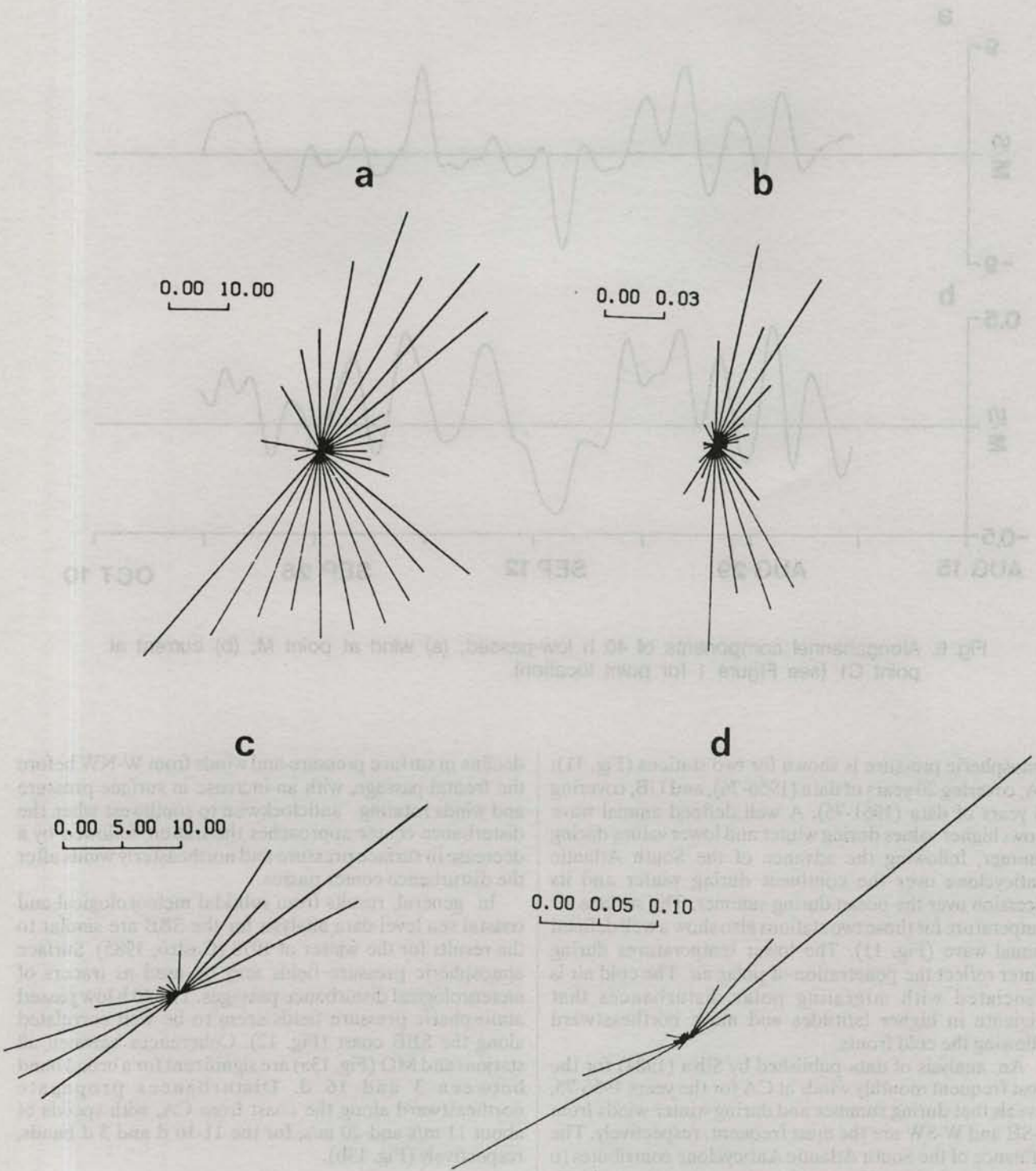
Fig. 7. Roses for 40 h low-passed wind at point M: (a) mean speed (m/s), (b) percent population; and 40 h low-passed current at point C1: (c) mean speed (cm/s), (d) percent population (see Figure 1 for point location).
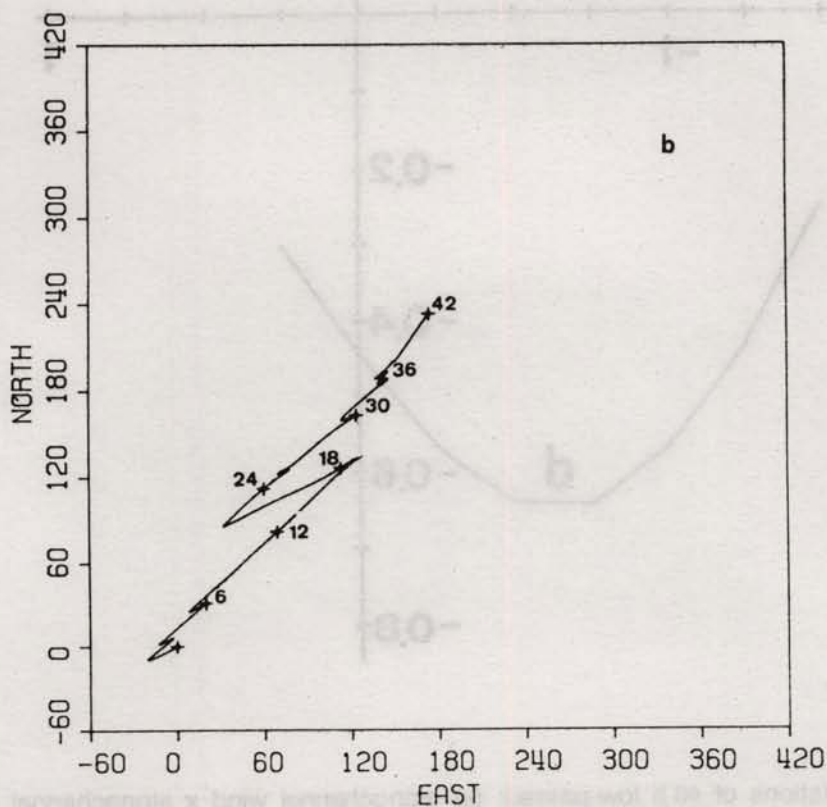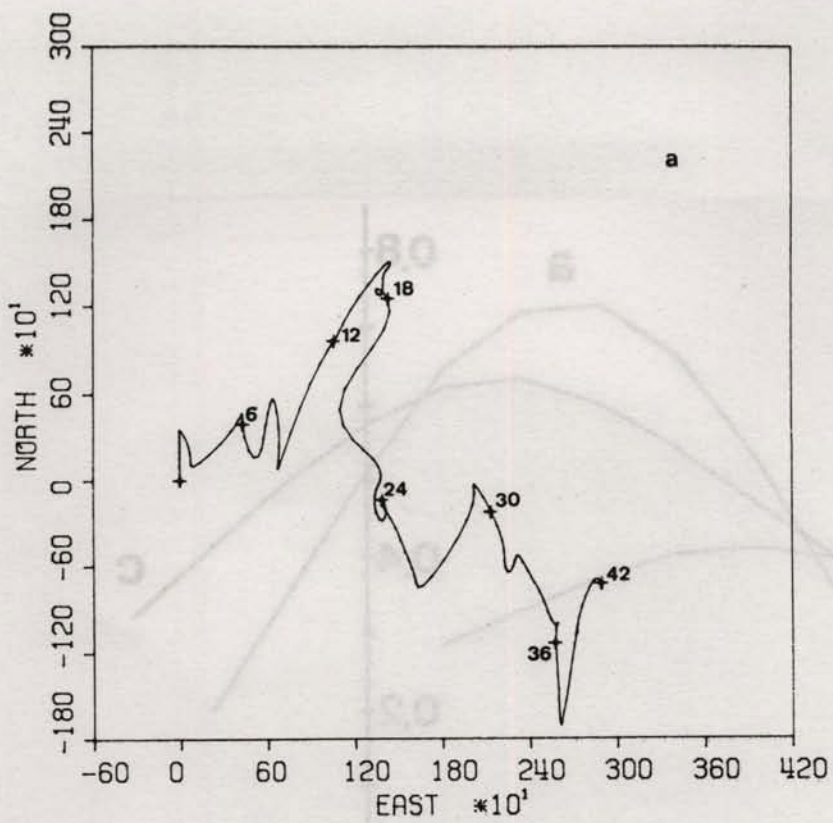
Fig. 8. Progressive vector diagrams for 40 h low-passed: (a) wind at point M; (b) current at point C1 (see Figure 1 for point location). Numbers represent days from start time.
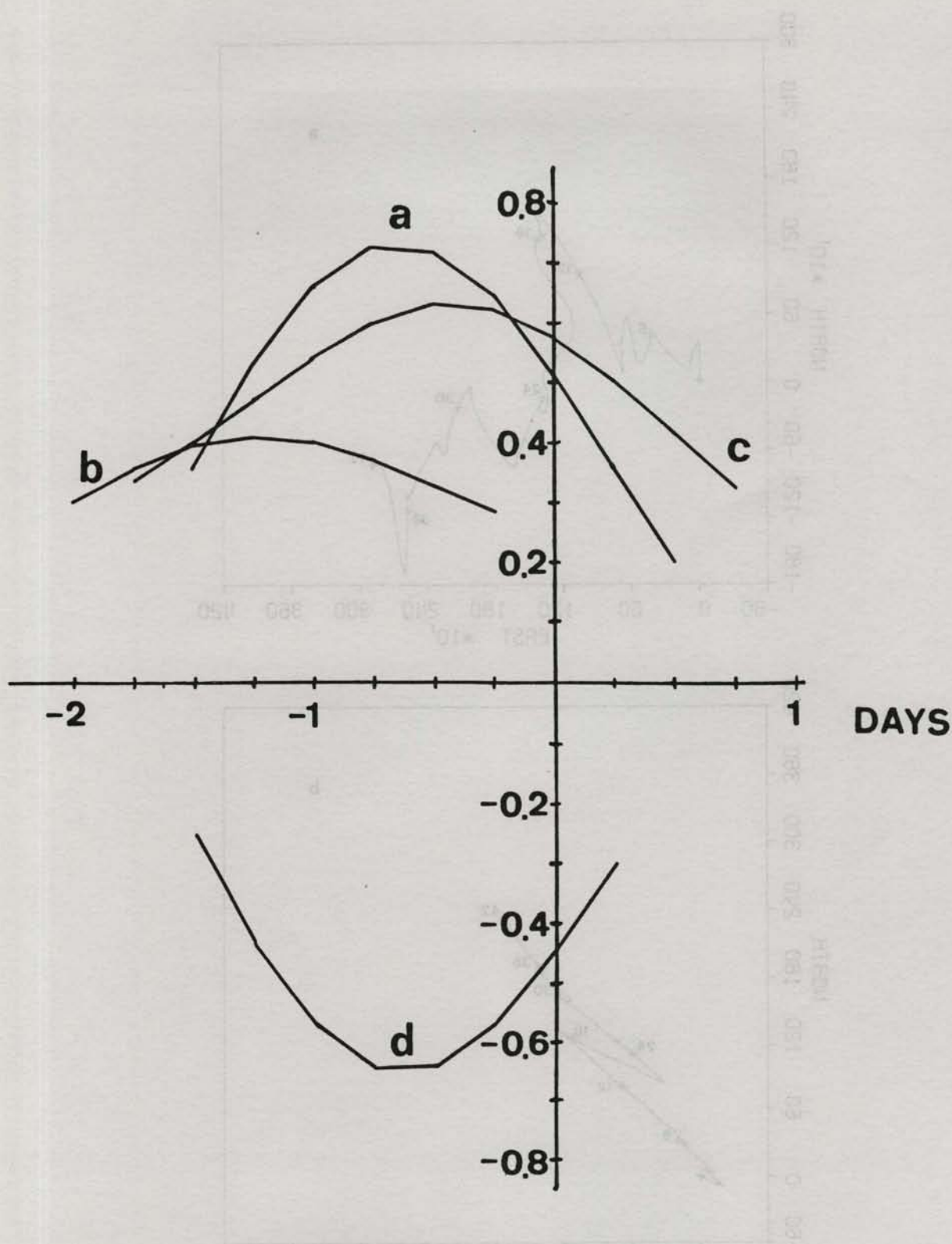
Fig. 9. Cross-correlations of 40 h low-passed: (a) alongchannel wind x alongchannel current; (b) alongchannel wind x sea level; (c) alongchannel current x sea level; (d) cross-channel wind x alongchannel current. Wind from point M, sea level from point T and current from point C1 (see Figure 1 for point location).
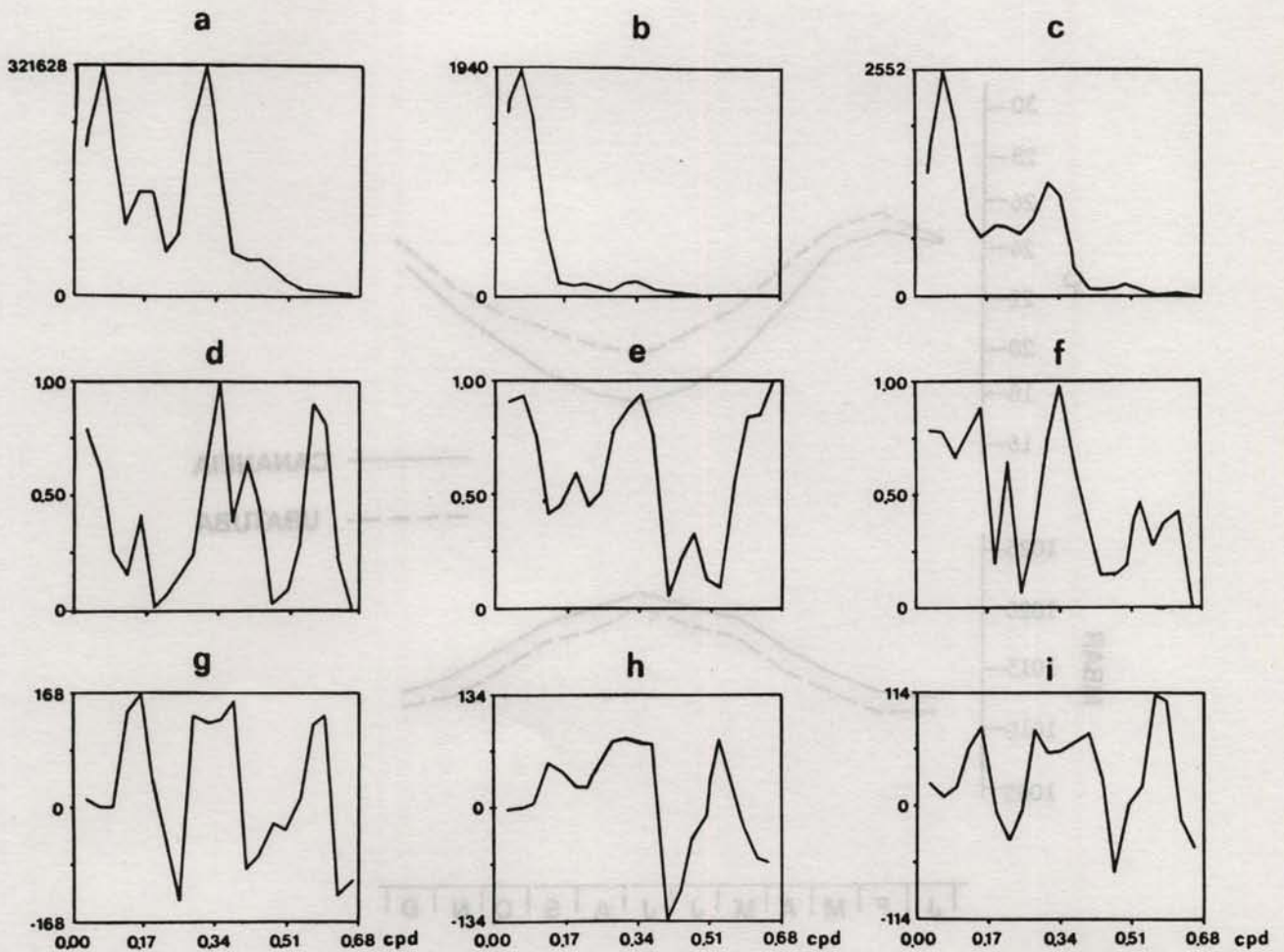
Fig. 10. Autospectra of 40 h low-passed: (a) wind, (b) current and (c) sea level. Coherences and phases for 40 h low-passed: alongchannel wind x alongchannel current (d and g), alongchannel wind x sea level (e and h), and alongchannel current x sea level (f and i). Wind from point M, sea level from point T and current from point C1 (sea Figure 1 for point location). The number of degrees of freedom is 7.
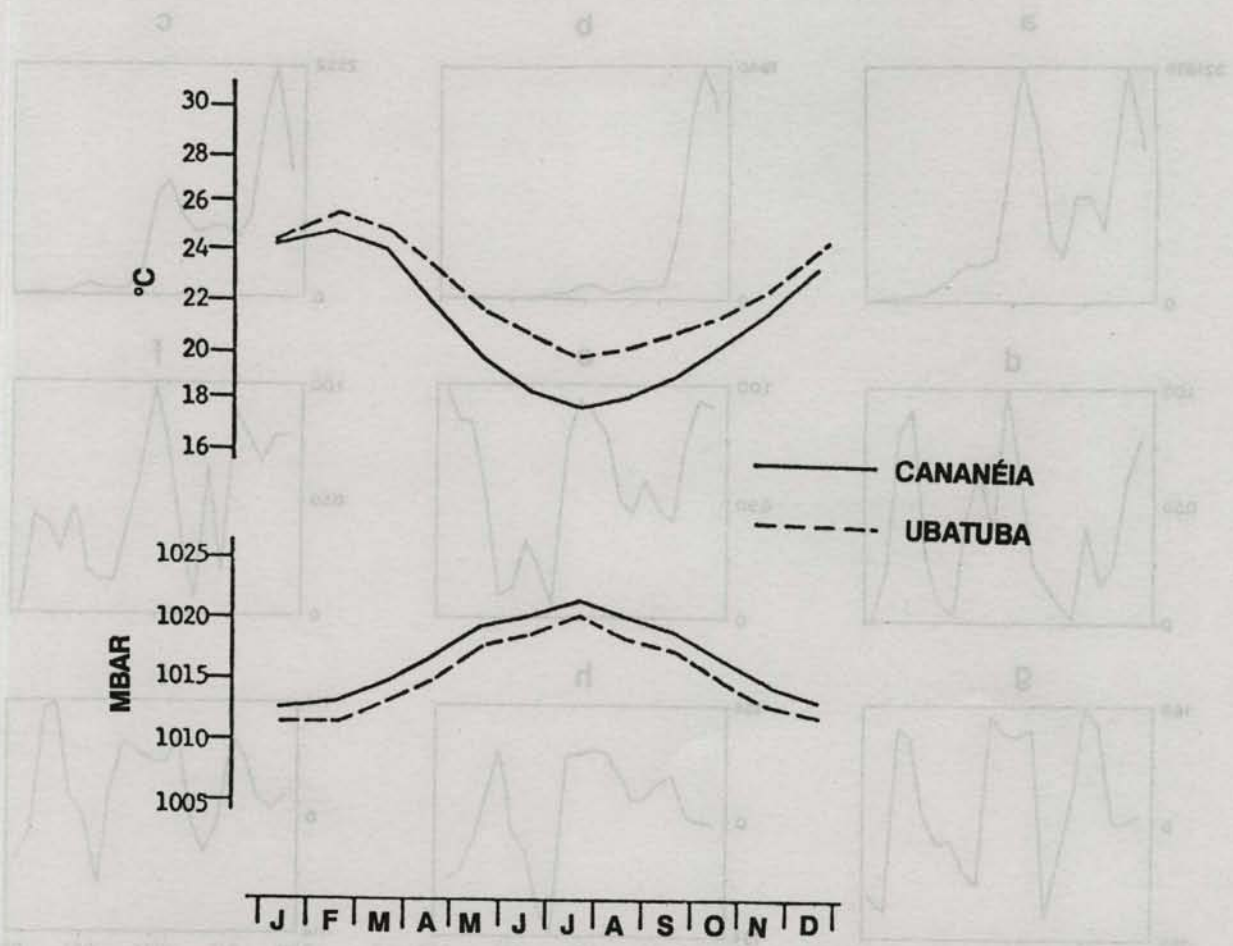
Fig. 11. Monthly mean surface atmospheric pressure and surface air temperature at: (a) Cananéia and (b) Ubatuba.
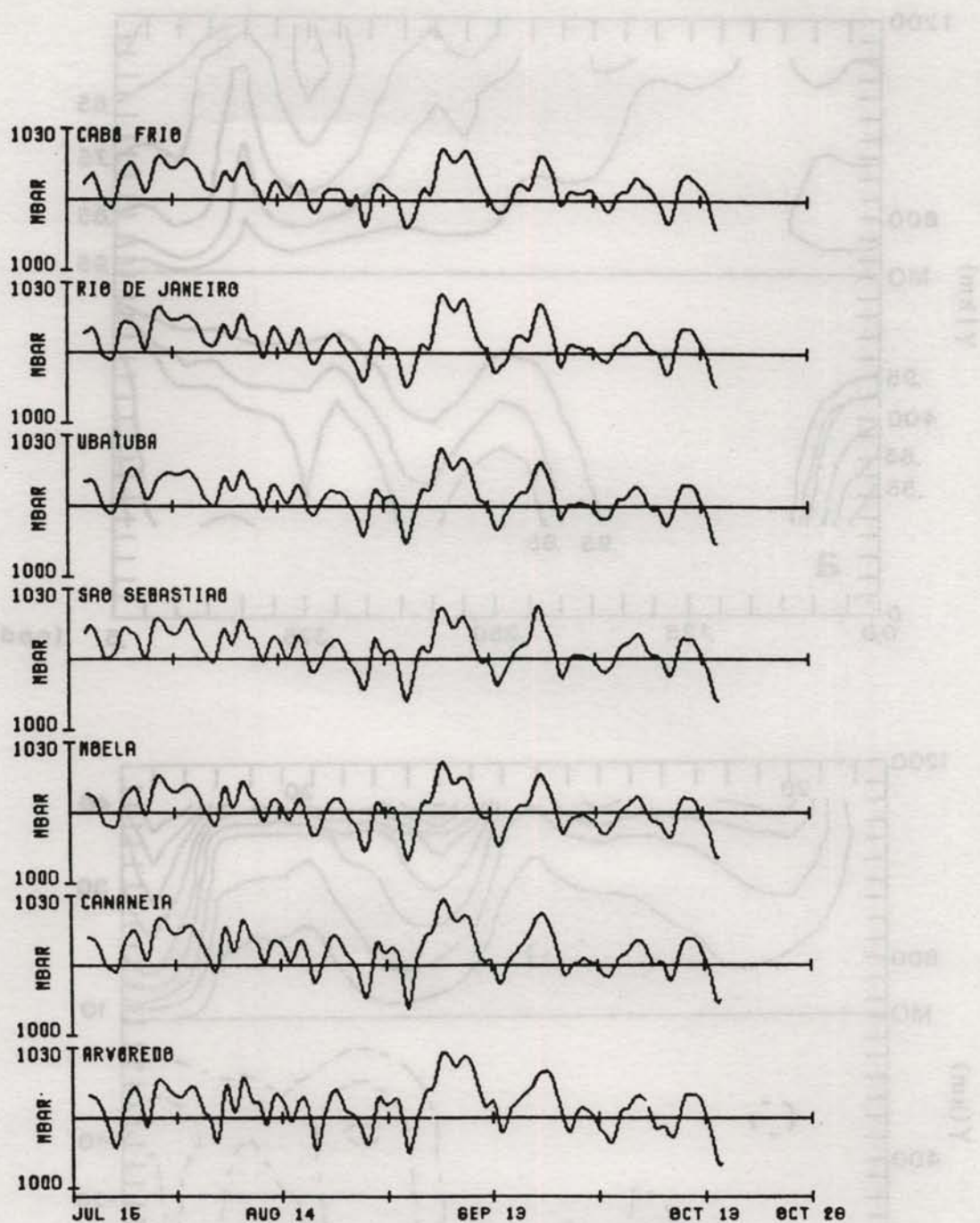
Fig. 12. 40 h low-passed surface atmospheric pressure time series along the South Brazil Bight coast for winter/1979.
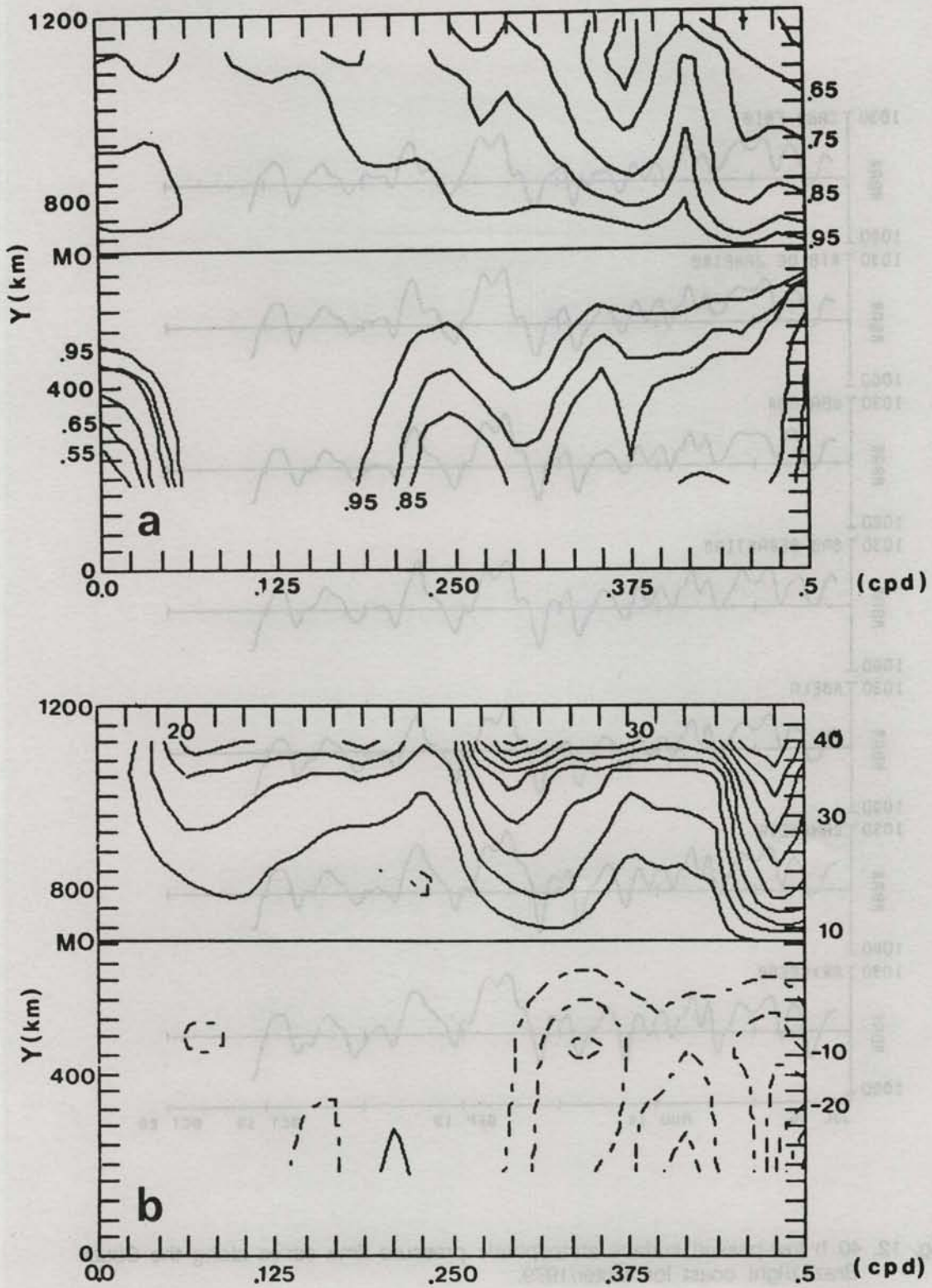
Fig. 13. Contours of cross-spectra between 40 h low-passed surface atmospheric pressure in MO and 40 h low-passed surface atmospheric pressure in AR, CA, MO, SS, UB, RJ and CF on frequency-alongshore distance planes: (a) coherence; and (b) phase. Number of degrees of freedom is 11.2 and 95% significance limit for null hypothesis in coherence is 0.48. Data for winter/1979.
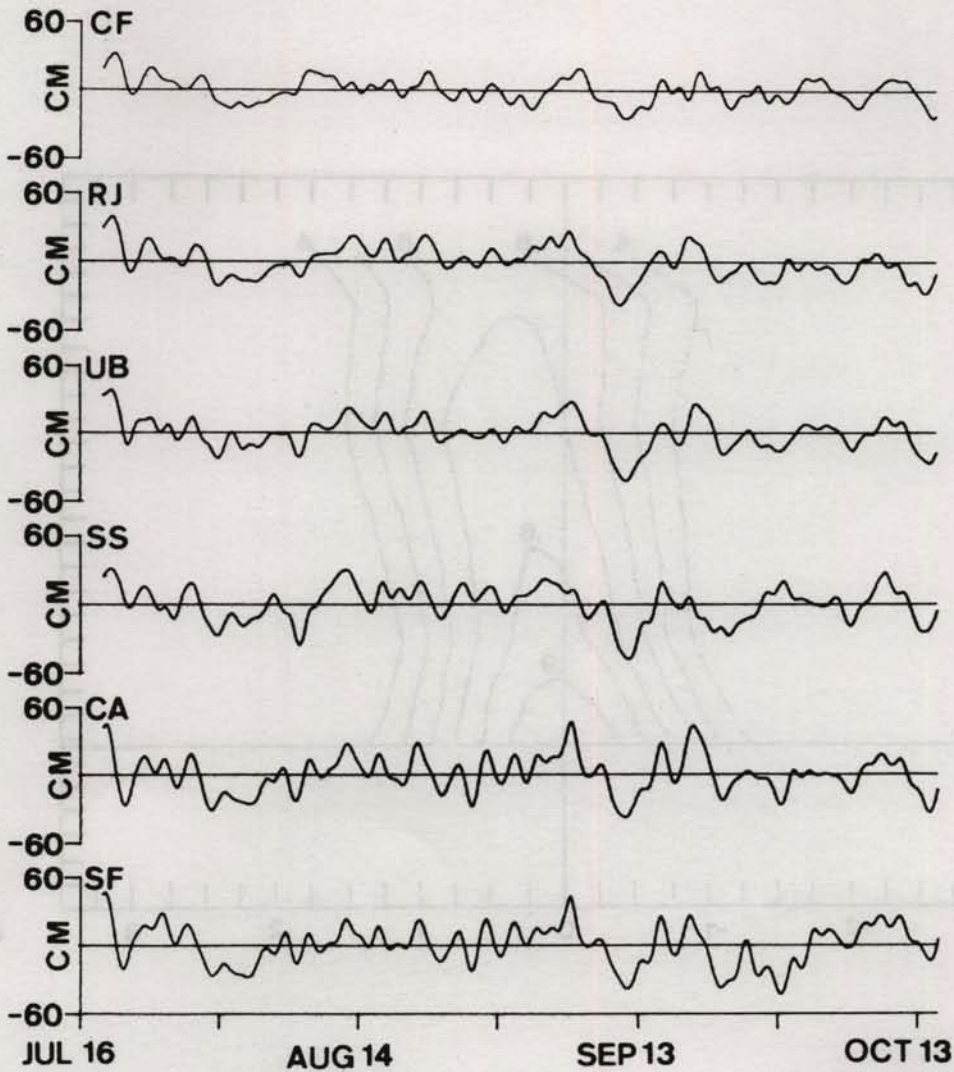
Fig. 14. 40 h low-passed sea level time series along the South Brazil Bight coast for winter/1979.
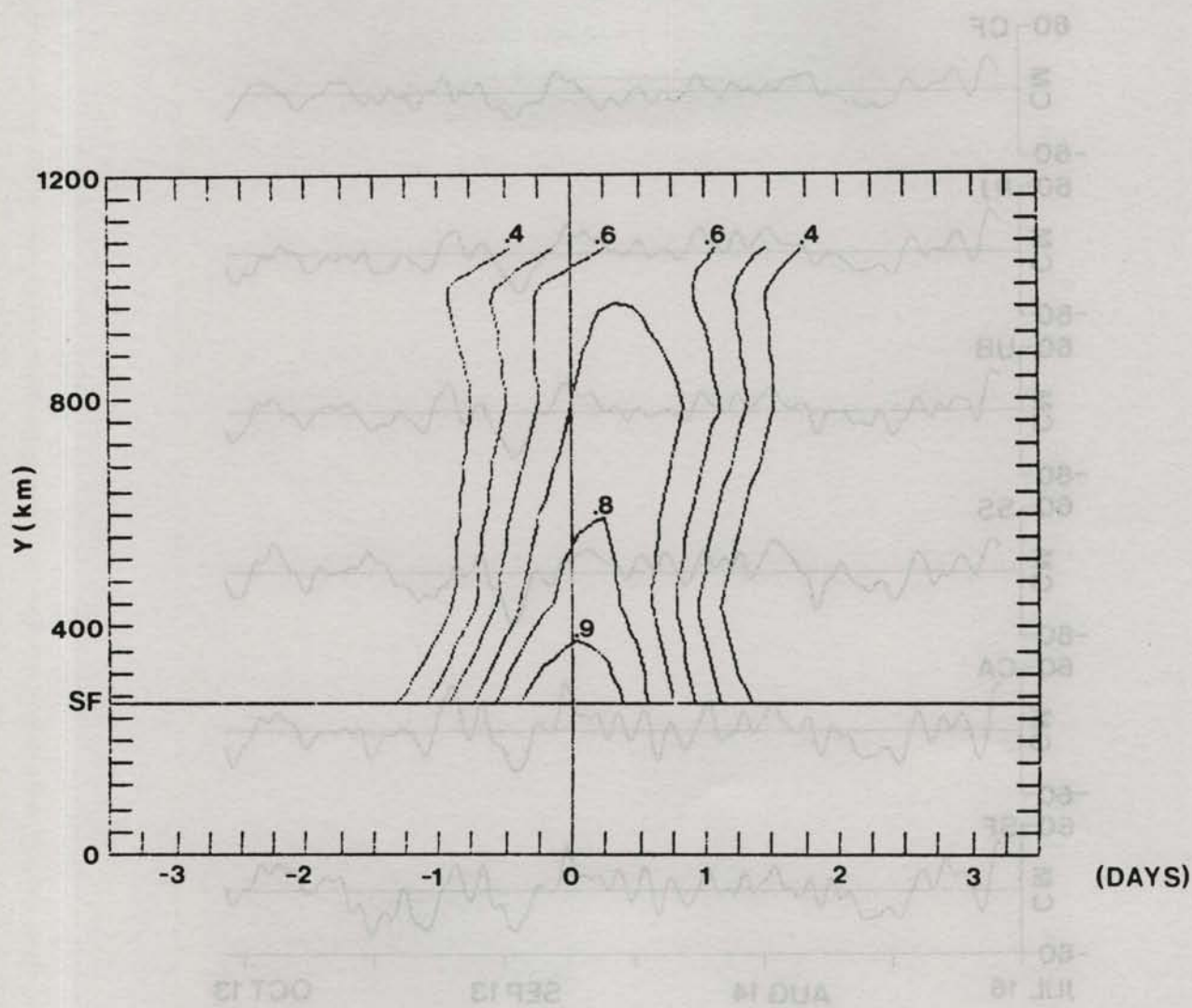
Fig. 15. Contours of space and time lagged cross-correlations of 40 h low-passed sea level in SF with 40 h low-passed sea level at each of the following stations: SF, CA, SS, UB, RJ and CF, for winter/1979. Correlations higher than 0.37 are significant to a 99% level of confidence.
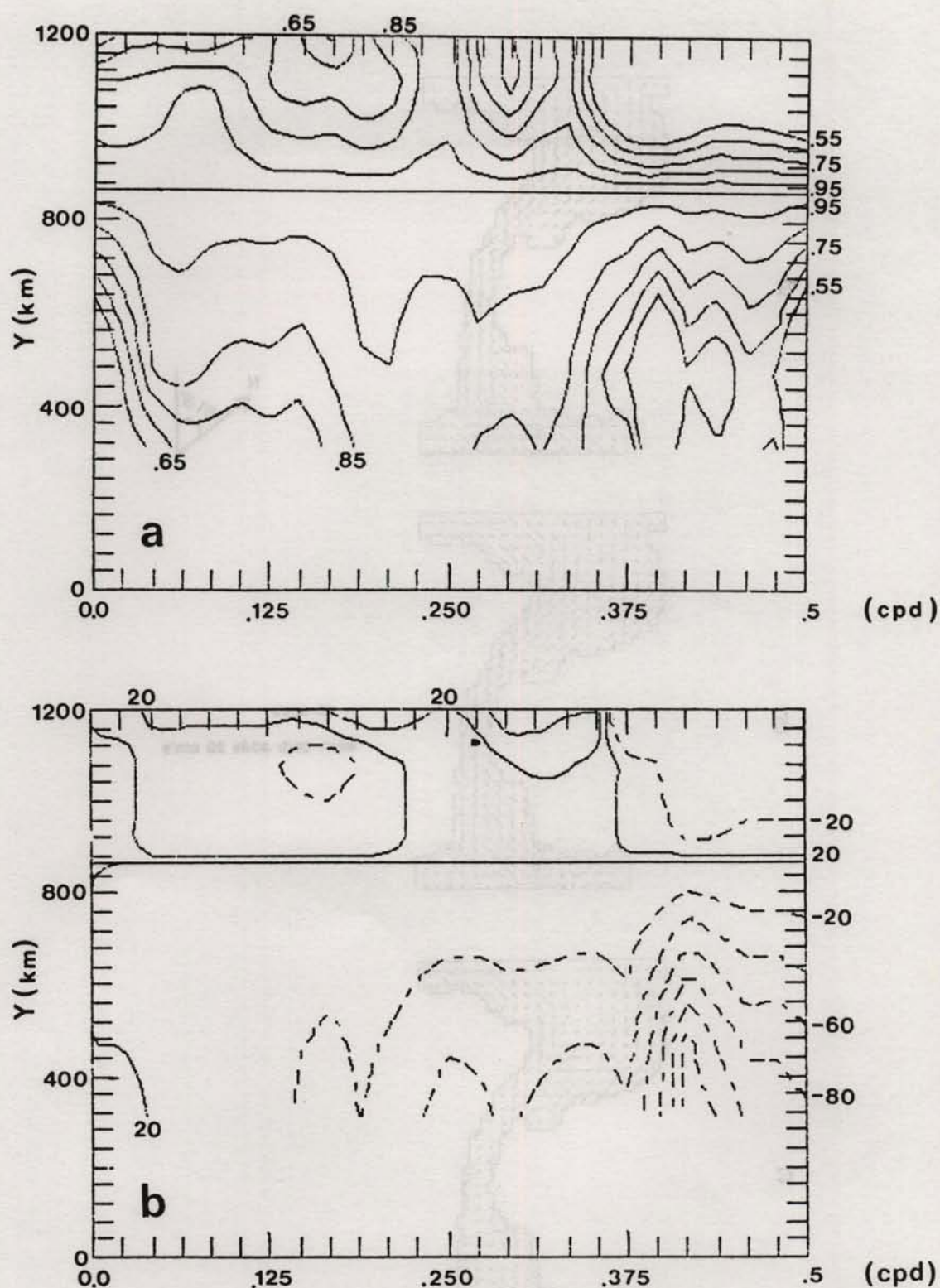
Fig. 16. Contours of cross-spectra between 40 h low-passed sea level in UB and 40 h low-passed sea level in SF, CA, SS, UB, RJ and CF on frequency-alongshore distance planes: (a) coherence; and (b) phase. Number of degrees of freedom is 11.2 and 95% significance limit for null hypothesis in coherence is 0.48. Data for winter/1979.
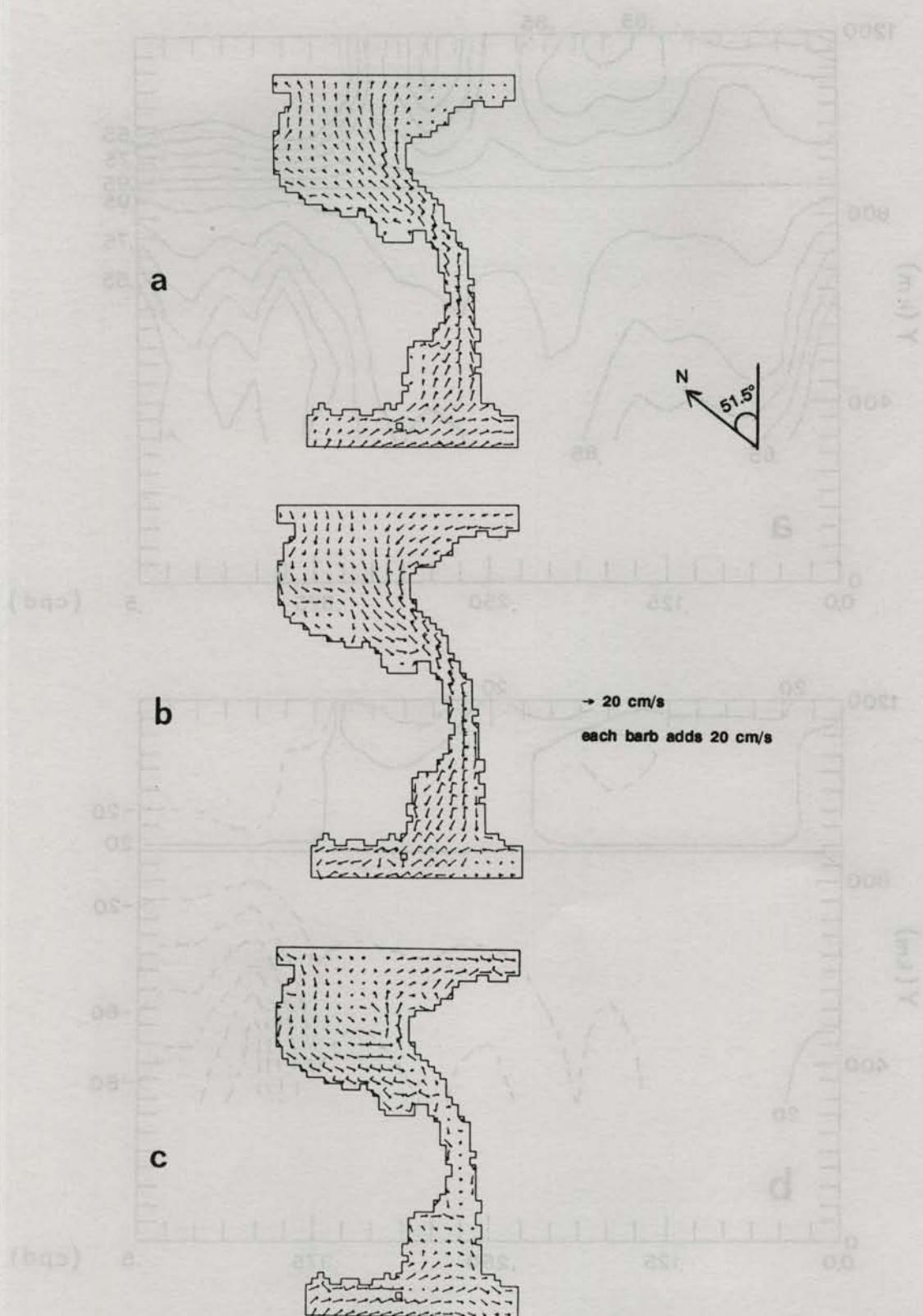
Fig. 17. Currents in the CSS (vertical mean) generated by a wind forced nested numerical model: (a) northeastward regime, (b) southwestward regime, and (c) double cell regime (adapted from Castro, 1985).

Discussion and conclusions

Currents in the CSS were mainly due to the wind, being the variance of tidal currents comparatively small. Thus, current oscillations were mainly subtidal. Water level, on the other hand, was dominated by tidal oscillations, while wind components were affected equally by both tidal and subtidal oscillations.

The best correlation between low-passed current and wind corresponded to a time lag of 12-18 h, wind leading. After low- passing the wind signal should be dominated by synoptic scale oscillations, which have scale length of about 1000 km and propagate equatorward in the SBB. Thus, wind driven currents at the CSS probably are not totally forced locally, but should be connected to the inner shelf circulation in a broader region encompassing the channel. Three typical current distributions in the CSS are shown in Figure 17: equatorward or poleward currents (Fig. 17a,b) when the main wind component is equatorward or poleward, respectively; and a double cell circulation, formed by an anticyclonic gyre in the northern half of the channel, and a cyclonic gyre in the southern part of the channel. Currents within the two opposing gyres are relatively strong, while currents in the central narrow portion of the channel are very weak, in contrast with the equatorward or poleward regimes, when higher velocities are found along the maximum depth axis of the channel. The results shown in Figure 17a-c are from nested numerical model experiments of wind driven circulation in the SBB (Castro, 1985). The double cell type of circulation would hardly be generated by local wind alone, since the two gyres should have extensions outside the channel. Thus, in general, wind driven currents in the CSS are part of the inner shelf circulation in a broader region encompassing the channel, and are not necessarily locally forced.

Maximum alongchannel currents were 0.45 m/s southwestward and 0.54 m/s northeastward. In the 40 h low passed data there is high correlation between the alongchannel components of wind and current, wind leading by 12-18 h. Low-passed alongchannel wind and sea level were only marginally correlated. Since most of the low-frequency dynamics might not be locally forced, and since there is high correlation between wind and coastal sea level in the SBB outside the CSS, it is likely that local effects, like topography and the shape of the channel, affect sea level oscillations that are propagating along the SBB coast.

Wind, current and sea level are dominated by 11-16 d and 3 d oscillations in the subtidal band, with significant coherence between signals. Alongchannel wind leads current and sea level by 16 and 25 h, respectively, in the 3 d band. The lag between wind and sea level agrees with the frictional response time found numerically for the region (Castro, 1985). The lag between current and sea level is not well understood, and has been observed in other inner shelf areas of the world, like the South Atlantic Bight (Schwing *et al.,* 1983).

The problem of low intensity of tidal currents versus high variance of sea level in the tidal band will be deferred for a latter paper.

Finally, a word of caution for environmentalists who might try to extrapolate in space and time the results presented in this paper: currents in the CSS may be highly variable in space and time, specially during periods of weak winds.

Resumo

Dados simultâneos de vento, corrente e nível do mar no Canal de São Sebastião (CSS), e de pressão atmosférica e nível do mar na Plataforma Continental Sudeste (PCS), coletados durante o inverno de 1979, foram analisados e comparados. Todas as séries de tempo foram previamente filtradas utilizando um filtro passa baixa com corte em 40 h. As correntes no CSS foram predominantemente para nordeste, em associação com ventos vindos do sul juntamente com sistemas meteorológicos frontais. Reversões de corrente ocorreram entre as passagens das perturbações atmosféricas. Foram significativas as correlações entre as componentes paralelas ao canal do vento e da corrente, havendo um deslocamento de 12-18 h, com liderança do vento; e também entre a componente paralela ao canal da corrente e o nível do mar, com deslocamento de 6-12 h, corrente liderando. A maior parte da variância nas séries de tempo para o CSS está concentrada em duas faixas de freqüência: 11-16 d e 3 d. Essas duas faixas também apresentam valores significativos quando calculadas entre as componentes paralelas ao canal do vento e da corrente, e o nível do mar no CSS. Esses três últimos sinais estavam quase em fase na faixa de 11-16 d; e havia uma liderança de 16 h (25 h) pelo vento sobre a corrente (nível do mar) na faixa de 3 d. Existem várias indicações que em baixas frequências as correntes no CSS não são forçadas localmente em sua totalidade.

Acknowledgement

References

CASTRO Fo., B. M. de 1985. Subtidal response to wind forcing in the South Brazil Bight during winter. Ph.D. dissertation. University of Miami, RSMAS, 203p.

_____; MIRANDA, L. B. de & MIYAO, S. Y. 1987. Condições hidrográficas na plataforma continental ao largo de Ubatuba: variações sazonais e em média escala. Bolm Inst. oceanogr., S Paulo, *35*(2):135-151.

EMILSSON, I. 1962. As correntes marítimas no Canal de São Sebastião. Ciênc. Cult., S Paulo, *14*:269-270.

JENKINS, G. M. & WATTS, D. G. 1968. Spectral analysis and its applications. San Francisco, Holden Day. 525p.

KVINGE, T. 1967. On the special current and water level variations in the Channel of São Sebastião. Bolm Inst. oceanogr., S Paulo, *16*:23-38.

SILVA, J. F. 1984. Dados climatológicos de Cananéia e Ubatuba (Estado de São Paulo). Bolm climatol., Inst. oceanogr. Univ. S Paulo, (5):1-18.

SCWING, F. B.; KJERFVE, B. & SNEED, J. E. 1983. Nearshore coastal current on the South Carolina continental shelf. J. geophys. Res., *88* (C8):4719-4729.